Chromium Activates Glucose Transporter 4 Trafficking and Enhances Insulin-Stimulated Glucose Transport in 3T3-L1 Adipocytes via a Cholesterol-Dependent Mechanism

Guoli Chen,* Ping Liu,* Guruprasad R. Pattar, Lixuan Tackett, Padma Bhonagiri, Andrew B. Strawbridge, and Jeffrey S. Elmendorf

Departments of Cellular and Integrative Physiology (G.C., P.L., G.R.P., L.T., P.B., A.B.S., J.S.E.) and Biochemistry and Molecular Biology (J.S.E.), Indiana University School of Medicine, Center for Diabetes Research, Indianapolis, Indiana 46202

Evidence suggests that chromium supplementation may alleviate symptoms associated with diabetes, such as high blood glucose and lipid abnormalities, yet a molecular mechanism remains unclear. Here, we report that trivalent chromium in the chloride ($CrCl_3$) or picolinate (CrPic) salt forms mobilize the glucose transporter, GLUT4, to the plasma membrane in 3T3-L1 adipocytes. Concomitant with an increase in GLUT4 at the plasma membrane, insulin-stimulated glucose transport was enhanced by chromium treatment. In contrast, the chromium-mobilized pool of transporters was not active in the absence of insulin. Microscopic analysis of an exofacially Myc-tagged enhanced green fluorescent protein-GLUT4 construct revealed that the chromium-induced accumulation of GLUT4-containing vesicles occurred adjacent to the inner cell surface membrane. With insulin these transporters physically incorporated into the plasma membrane. Regulation of GLUT4 translocation by chromium did not involve known insulin signaling proteins such as the insulin receptor, insulin receptor substrate-1, phosphatidylinositol 3-kinase, and Akt. Consistent with a reported effect of chromium on increasing membrane fluidity, we found that chromium treatment decreased plasma membrane cholesterol. Interestingly, cholesterol add-back to the plasma membrane prevented the beneficial effect of chromium on both GLUT4 mobilization and insulin-stimulated glucose transport. Furthermore, chromium action was absent in methyl-β-cyclodextrin-pretreated cells already displaying reduced plasma membrane cholesterol and increased GLUT4 translocation. Together, these data reveal a novel mechanism by which chromium may enhance GLUT4 trafficking and insulin-stimulated glucose transport. Moreover, these findings at the level of the cell are consistent with *in vivo* observations of improved glucose tolerance and decreased circulating cholesterol levels after chromium supplementation. (*Molecular Endocrinology* 20: 857–870, 2006)

CHROMIUM (Cr), an essential transition metal, may be an important addition to type 2 diabetes treatment choices because it is thought to play a role in glucose metabolism by potentiating the action of insulin. Encouraging findings in animal and human studies (1–3) have led many investigators to hypothesize that dietary Cr supplementation may help to control type 2 diabetes. Cr exists in several valence states, the most prevalent oxidation states being hexavalent Cr (which is associated with industrial exposure and toxicity) and trivalent Cr (which is stable and the biologically active form). Cr supplements are available as trivalent Cr in the chloride ($CrCl_3$) or picolinate (CrPic) salt forms. Animal studies have shown that a deficiency in dietary Cr can result in an inability to remove glucose efficiently from the bloodstream (4). Evidence also suggests that diet-induced insulin resistance in experimental animals can be improved by Cr supplementation (5). In humans, there also seems to be an association between insulin resistance and Cr status (6).

Glucose homeostasis is achieved by the ability of insulin to efficiently stimulate the storage and metabolism of glucose. In muscle and adipose tissues, insulin stimulates the removal of circulatory glucose by regulating the subcellular trafficking of the glucose transporter GLUT4. In the basal state, GLUT4 cycles

continuously between the plasma membrane and an intracellular compartment(s), with the majority of the transporter residing within the cell interior (7). Activation of the insulin receptor (IR) by insulin triggers a large increase in the rate of GLUT4 vesicle exocytosis and a smaller but important decrease in the rate of internalization by endocytosis (8–10). The overall insulin-dependent shift in the dynamics of GLUT4 vesicle trafficking results in a net increase of GLUT4 protein levels in the plasma membrane that amplify the cellular uptake of glucose.

The exact mechanism whereby Cr participates in the functions of insulin has not been elucidated, but theories range from direct interaction of Cr with insulin (11) to a role of Cr in increasing IR number (12), as well as increasing IR tyrosine kinase activity already engaged by insulin (13). It has been demonstrated that a naturally occurring oligopeptide, low-molecular-weight Cr-binding substance (termed "chromodulin"), binds chromic ions in response to an insulin-mediated chromic ion flux, and the metal-saturated oligopeptide then binds to an insulin-stimulated IR, activating the receptor's tyrosine kinase activity as much as 8-fold in the presence of insulin (13, 14). The chromodulin-mediated autoamplification of the IR's tyrosine kinase activity would be expected to enhance the regulated movement of GLUT4 and, subsequently, enhance glucose disposal. This anticipated biological outcome has been observed (3), but signaling molecules responsible for the translocation have not yet been evaluated.

Another aspect of Cr action that may explain, at least in part, its enhancement of insulin sensitivity is its effect on increasing membrane fluidity and the rate of insulin internalization (15). Although insulin-stimulated GLUT4 translocation does not appear dependent upon insulin first being transported into the cell (16), studies suggest that IR internalization may compartmentalize and efficiently promote interaction with its substrate(s) associated with internal membranes (17–19). In agreement with membrane fluidity changes as a basis for the effect of Cr, moderate increases in plasma membrane fluidity have been documented to increase glucose transport (20, 21). Furthermore, it has been shown that basal glucose transport is not fully active in fat cells and that it can be increased further by augmenting membrane fluidity (20). Consistent with membrane fluidity influencing insulin responsiveness, insulin-stimulated glucose transport is decreased when fluidity diminishes (21). Interestingly, recent data suggest that the antidiabetic drug metformin enhances insulin action by increasing membrane fluidity (22, 23). As has been observed after Cr treatment (3), metformin treatment has been reported to increase GLUT4 translocation (24–26).

The present work set out to test whether the beneficial effects of Cr on insulin action resulted from changes in plasma membrane properties. Our data demonstrate that plasma membrane cholesterol content was diminished in cells exposed to Cr and that exogenous cholesterol replenishment rendered the enhancement of insulin action by Cr ineffective. Interestingly, in the absence of insulin, the Cr-mobilized pool of GLUT4 was ineffective in transporting glucose. However, the extent of insulin-stimulated glucose transport was amplified by this Cr-mobilized pool of transporters.

RESULTS

Cr Triggers the Redistribution of GLUT4 to the Plasma Membrane in Adipocytes

Our preliminary treatment parameters were selected based on *in vitro* data showing trivalent Cr in the chloride and picolinate salt formulations, ranging from 1 μM to 20 μM, enhanced glucose uptake and membrane fluidity in cultured mouse and rat skeletal muscle cells (15, 27). Incubation of 3T3-L1 adipocytes with 10 μM $CrCl_3$ or 10 μM CrPic for 16 h increased the basal and insulin-stimulated level of GLUT4 in the plasma membrane as assessed by GLUT4 immunofluorescence of highly purified plasma membrane sheets (Fig. 1A). Digital image processing showed the basal-state plasma membrane levels of GLUT4 after $CrCl_3$ and CrPic pretreatments were increased 44% ($P < 0.001$) and 35% ($P < 0.001$), respectively. The insulin-stimulated plasma membrane level of GLUT4 was increased 151% ($P < 0.005$) and this stimulation was amplified by both $CrCl_3$ and CrPic pretreatments by 43% ($P < 0.05$) and 39% ($P < 0.05$), respectively. To confirm the effect of Cr on the accumulation of GLUT4 in isolated plasma membrane sheets, we used differential centrifugation to isolate plasma membrane from 3T3-L1 adipocytes. Plasma membrane fractions prepared from cells treated with insulin displayed a characteristic increase in GLUT4 compared with plasma membrane fractions prepared from untreated cells (Fig. 1B, compare lanes 1 and 2). Consistent with the microscopic analysis, immunoblot analysis showed that Cr treatment for 16 h increased the basal-state level of GLUT4 in the plasma membrane (Fig. 1B, compare lanes 1, 3, and 5), and the insulin effect was enhanced in the presence of Cr (Fig. 1B, compare lanes 2, 4, and 6). A constant finding with plasma membrane preparation via subcellular fractionation (Figs. 1B and 6B) was that the chromium-induced increase in the basal-state plasma membrane level of GLUT4 was similar to that induced by insulin alone; however, this was not the case in isolated plasma membrane sheets where the chromium effect on the basal-state plasma membrane level of GLUT4 was less than that of insulin. In contrast to plasma membranes obtained with the sheet assay, which are highly purified, the fractions isolated by centrifugation are likely contaminated, to some extent, with cytosol and intracellular vesicles (28). Therefore, although chromium appears to be mobilizing GLUT4 to the plasma membrane, the majority of it may not be physically
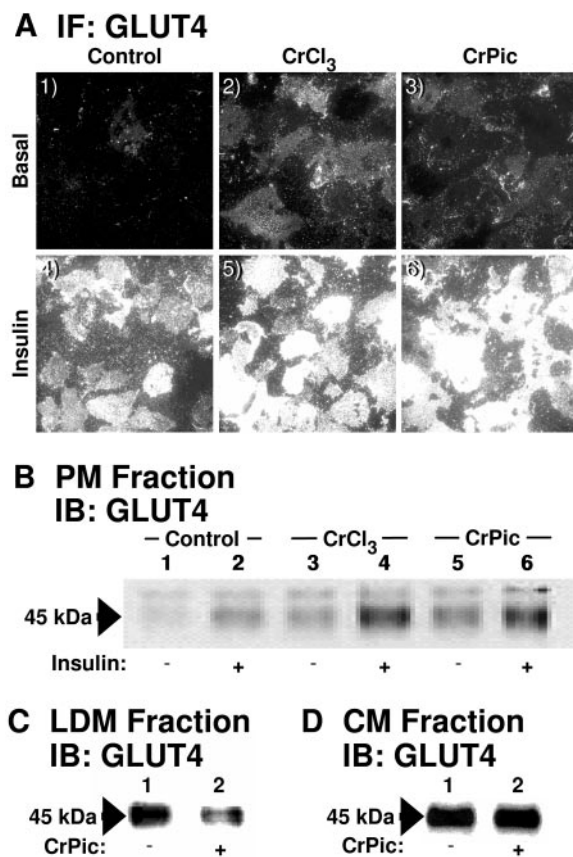
Fig. 1. Cr Stimulates GLUT4 Translocation

3T3-L1 adipocytes were treated with 10 μM CrCl$_3$ or 10 μM CrPic in serum-free DMEM for 16 h. During the last 30 min of incubation, the cells were either left unstimulated (Basal) or stimulated with 1 nM insulin. A, Representative plasma membrane (PM) sheet GLUT4 images are shown from five to eight experiments. B, PM; C, low-density microsome (LDM); and D, crude membrane (CM) fractions immunoblotted (IB) for GLUT4. These are representative immunoblots (IB) from three to five independent experiments. IF, Immunofluorescence.

incorporated into the cell surface. Nonetheless, these microscopic and biochemical data clearly show that chromium elicits an insulin-like accumulation of GLUT4 at the plasma membrane in 3T3-L1 adipocytes. As shown in Fig. 1C, this accumulation elicited by CrPic treatment occurs concomitant with a loss of GLUT4 protein in the low-density microsome fraction. Also, chromium treatment did not affect total GLUT4 protein levels detected in crude total membrane fractions (Fig. 1D).

**Key Insulin Signal Transduction Events Are Not Stimulated by Cr**

There are several possible mechanisms that could account for the increased GLUT4 translocation by Cr. We first explored whether known proximal insulin signal transduction events, including IR autophosphory-

lation, IR substrate-1 (IRS-1), Cbl tyrosine phosphorylation, and Akt phosphorylation were involved. Given that the most popular form of chromium in dietary supplements is CrPic (29), here and most of the subsequent analyses aimed at understanding the molecular mechanism of Cr action used CrPic. Insulin stimulation resulted in increased tyrosine phosphorylation of the IR β-subunit, IRS-1, and Cbl at 5 min (Fig. 2, A–C; compare lanes 1 and 3) or at 2-, 15-, 30-min treatment intervals (data not shown). In contrast to the effect of insulin, the overnight CrPic pretreatment associated with insulin-like activity had no effect on the phosphorylation of these proteins in the absence or presence of insulin (Fig. 2, A–C; compare lanes 1 and 2, and 3 and 4). Immunoblotting of those same membranes with anti-IR β-subunit, IRS-1, and Cbl antibodies demonstrated the presence of equal amounts of IR β-subunit, IRS-1 and Cbl (Fig. 2, A–C; lanes 5–8). In addition to immunoblotting cell lysates, we immunoblotted IR, IRS-1, and Cbl immunoprecipitates and these data confirmed that insulin, but not CrPic, increased the extent of tyrosine phosphorylation of these proteins (data not shown).

Although the signaling events distal to the Cbl cascade remain unclear, recognized molecules of the IRS-1 cascade involved in GLUT4 translocation are phosphatidylinositol 3-kinase (PI3K) and the Akt serine/threonine kinase. Akt-1 phosphorylation, which is indicative of activation, was assessed by using an antiphospho-Ser473 antibody that is specific for the serine phosphorylated Akt-1 isoform, whereas the phosphorylation of Akt-2 was determined by monitoring the mobility shift indicative of the phosphorylated and active enzyme (30). Insulin stimulated the phosphorylation of both Akt-1 (Fig. 2D, *left* immunoblot, compare lanes 1 and 3) and Akt-2 (Fig. 2D, *right* immunoblot, compare lanes 5 and 7). In contrast, exposure of cells to CrPic did not result in phosphorylation of either Akt isoform (Fig. 2D, compare lanes 1 and 2, and 5 and 6) or increase insulin's effect on these kinases (Fig. 2D, compare lanes 3 and 4, and 7 and 8).

To further assure ourselves that the classical insulin signaling pathway was not a target of Cr action, we sought to test the effect of PI3K inhibition on CrPic action. However, testing the role of PI3K with the PI3K inhibitors wortmannin or LY294002 was complicated by the 16-hr CrPic treatment. Moreover, because PI3K regulates endocytosis, a wortmannin-induced loss of CrPic action may reflect a loss of the endocytic uptake of CrPic and not CrPic-stimulated PI3K signaling. To circumvent these issues and assess the effect of CrPic on PI3K activity, we evaluated phosphatidylinositol 3,4,5-trisphosphate (PIP$_3$) generation as we have previously reported (31). Using a specific PIP$_3$ antibody (32, 33), microscopic analyses revealed very little endogenous PIP$_3$ localized at the plasma membrane in the absence or presence of CrPic treatment (Fig. 2E, panels 1 and 2). Strong nuclear PIP$_3$ labeling was observed in all cells (Fig. 2E), as previously documented (34). Consistent with PI3K activation by insu-
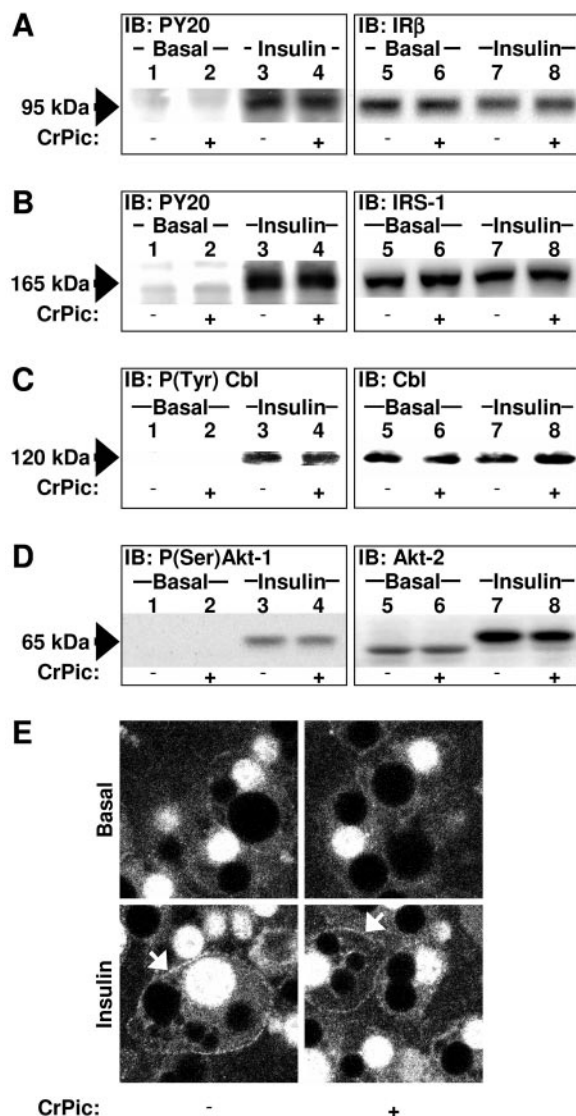
Fig. 2. Cr Treatment Does Not Enhance Basal or Insulin-Stimulated Phosphorylation States of the Insulin Receptor β-Subunit, IRS-1, Cbl, PI3K, or Akt
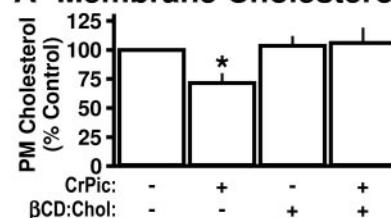
3T3-L1 adipocytes were left untreated (lanes 1 and 3) or treated with 10 μM CrPic (lanes 2 and 4) in serum-free DMEM for 16 h. During the last 5 min of incubation, the cells were either left unstimulated (Basal) or stimulated with 1 nM insulin. Whole-cell detergent lysates were generated and subjected to immunoblotting with antibodies to: A and B, phosphotyrosine (*left* immunoblots, lanes 1–4); A, IRβ (*right* immunoblot, lanes 5–8); B, IRS-1 (*right* immunoblot, lanes 5–8); C, P(Tyr) c-Cbl (*left* immunoblot, lanes 1–4) and Cbl (*right* immunoblot, lanes 5–8); D, P$^{(Ser)}$Akt (left immunoblot, lanes 1–4) and Akt-2 (*right* immunoblot, lanes 5–8) as described in *Materials and Methods*. These are representative immunoblots from three separate experiments. E, Shown are representative images of whole cell PIP$_3$ from three independent experiments.

lin, an increase in plasma membrane PIP$_3$ was apparent in insulin-stimulated cells (Fig. 2E, panel 3), an amplification of this by CrPic exposure was not evident (Fig. 2E, compare panels 3 and 4).
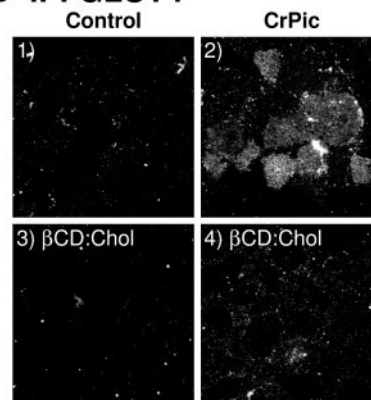
Cr-Induced GLUT4 Translocation Is Coupled to Plasma Membrane Cholesterol Loss

Recently, we reported that moderate cholesterol depletion from the plasma membrane increases the basal-state plasma membrane level of GLUT4 (30). Given that Cr has been demonstrated to influence membrane fluidity (15), we next evaluated whether the insulin mimetic action of Cr may be coupled to changes in plasma membrane properties, in particular, cholesterol content. Exposure of the cells to CrPic for 16 h resulted in a 29% loss ($P < 0.05$) of plasma membrane cholesterol (Fig. 3A). This loss of cholesterol from the plasma membrane prompted us to ask whether Cr-induced GLUT4 translocation could be prevented by restoring the basal-state plasma membrane level of cholesterol. Here we used methyl-β-cyclodextrin (βCD) preloaded with cholesterol as we have previously reported (30) to replenish the depleted plasma membrane cholesterol. The reduction in plasma mem-

Fig. 3. Cr Diminishes Plasma Membrane Cholesterol and Cholesterol Replenishment Prevents Cr-Induced GLUT4 Translocation

3T3-L1 adipocytes were left untreated (−CrPic, panels 1 and 3) or treated with 10 μM CrPic (+CrPic, panels 2 and 4) in serum-free DMEM for 16 h, which did not (panels 1 and 2) or did contain (panels 3 and 4) 1 mM βCD preloaded with cholesterol. A, Cells were harvested, plasma membrane fractions were prepared, and membrane cholesterol content was determined as described in *Materials and Methods*. Results are expressed as percent of control. They represent the mean (±SE; *, $P < 0.05$) from three to four independent experiments. B, Representative plasma membrane (PM) sheet GLUT4 images are shown from three experiments. IF, Immunofluorescence.
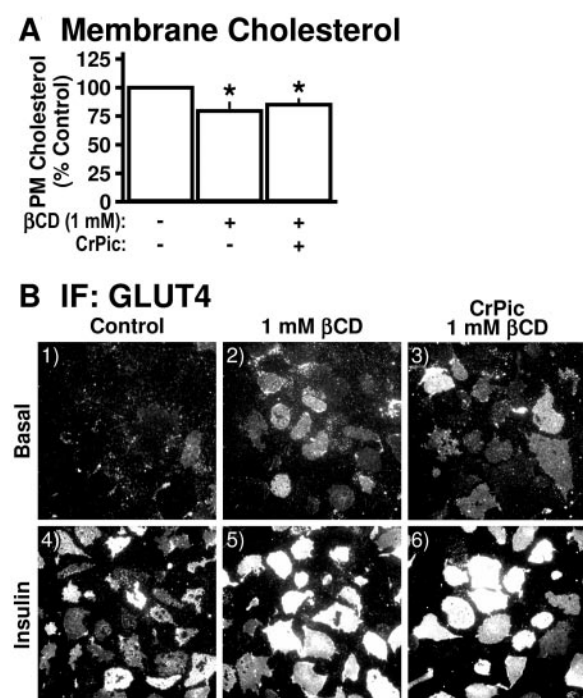
brane cholesterol induced by CrPic treatment was prevented in cells incubated in medium enriched with βCD preloaded with cholesterol (βCD:Chol) (Fig. 3A). The effect of βCD:Chol did not significantly alter the basal-state level of cholesterol content in the plasma membrane (Fig. 3A). The ability of CrPic to mobilize GLUT4 to the plasma membrane was prevented in cells incubated in βCD:Chol (Fig. 3B, compare panels 2 and 4) and the effect of βCD:Chol did not alter the basal-state level of GLUT4 in the plasma membrane (Fig. 3B, compare panels 1 and 3). These findings are consistent with previous work by our group (30) showing that reduction in plasma membrane cholesterol activates GLUT4 translocation.

To further explore this cholesterol dependency of Cr action, we next tested whether the Cr effect would be compromised in cells where membrane cholesterol was depleted by βCD pretreatment. As shown in Fig. 4A, exposure of 3T3-L1 adipocytes to 1.0 mM βCD for a total of 16.5 h lowered plasma membrane cholesterol by 20% ($P < 0.05$). Consistent with our previous findings, this βCD-induced loss of plasma membrane cholesterol was associated with an increase in basal

Fig. 4. Cells with a βCD-Induced Moderate Cholesterol Loss Are Unresponsive to Cr

Cells were pretreated without or with 1 mM βCD for 30 min and then left untreated or treated with 10 μM CrPic in serum-free DMEM in the continual presence of βCD for 16 h. After this 16.5-h period, cells were either left untreated or treated with 1 nM insulin for 30 min. A, Membrane cholesterol was determined and is presented as described in preceding legend. They represent the mean ($\pm$SE; *, $P < 0.05$) from three independent experiments. B, Representative plasma membrane (PM) sheet GLUT4 images are shown from three experiments. IF, Immunofluorescence.

(Fig. 4B, compare panels 1 and 2) and insulin-stimulated (Fig. 4B, compare panels 4 and 5) GLUT4 translocation. As shown in Fig. 3, CrPic treatment (16.5 h) in this experiment lowered plasma membrane cholesterol and increased GLUT4 translocation to the same extent as 1.0 mM βCD (data not shown). Interestingly, no further reduction in plasma membrane cholesterol was observed in βCD-treated cells exposed to CrPic (Fig. 4A). Consistent with Cr action being cholesterol dependent, no further augmentation of plasma membrane GLUT4 was observed in cells cotreated with βCD and CrPic (Fig. 4B, panels 3 and 6).
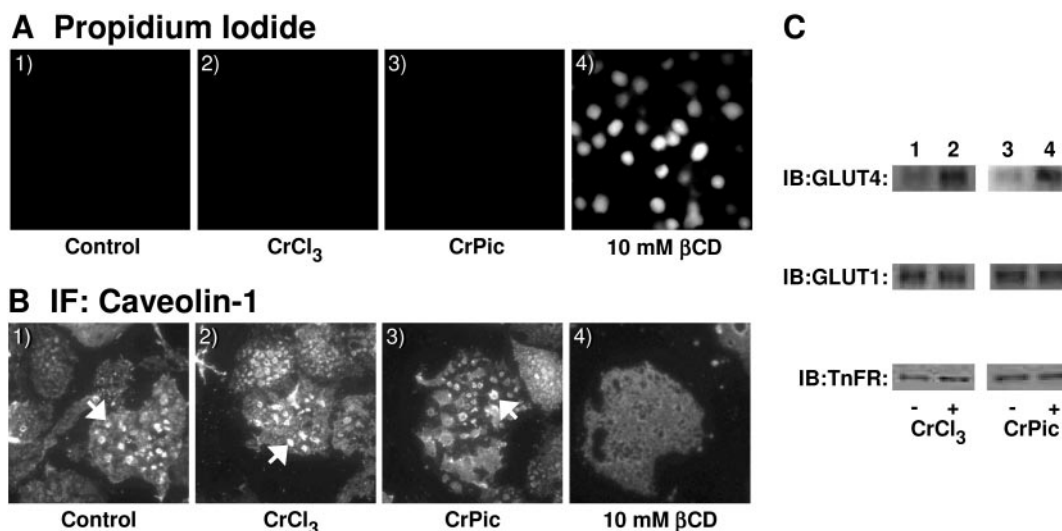
Although we previously observed that reductions in plasma membrane cholesterol below 50% are not associated with a loss of membrane integrity, whereas greater losses ($\geq$50%) are, a subsequent series of studies set out to visualize whether the chromium-induced loss of plasma membrane cholesterol affected membrane integrity. Whereas 3T3-L1 adipocytes exposed to a dose of βCD (10 mM) previously reported to diminish plasma membrane cholesterol by approximately 65% (30) displayed nuclear propidium iodide staining (Fig. 5A, compare panels 1 and 4), membrane integrity appeared intact in cells exposed to 10 μM CrCl$_3$ or 10 μM CrPic (Fig. 5A, panels 2 and 3). Although this assessment provided a global view of membrane permeability, we next measured the regional effects of Cr on cholesterol-enriched lipid raft microdomains. A large subset of lipid raft microdomains exists as plasma membrane caveolae that are clustered into higher-order structures in adipocytes, thus making them visible by light microscopy (30). High magnification of plasma membrane sheets from control cells and those incubated with Cr displayed an abundance of caveolin-enriched circular rosette structures (Fig. 5B, panels 1–3). In contrast, caveolin rosettes were not apparent in sheets prepared from cells exposed to 10 mM βCD (Fig. 5B, panel 4). Taken together, these results suggest that Cr promotes GLUT4 translocation via depletion of plasma membrane cholesterol without adverse effects on cell or caveolar integrity.

Recent studies have documented that cholesterol depletion greater than 50% reduces the rate of internalization of transferrin receptor (TnFR) by more than 85%, without affecting intracellular receptor trafficking back to the cell surface (35). In view of the inhibitory effect of extensive cholesterol depletion on endocytosis, we examined the effect of Cr on endocytosis by visualizing whether proteins that reside in different vesicle compartments than GLUT4 (GLUT1 and TnFR) accumulate in the plasma membrane with Cr treatment. Immunofluorescent microscopy of plasma membrane sheets (data not shown), and immunoblot analyses of subcellular fractions prepared by ultracentrifugation, show no changes in the basal-state plasma membrane level of the glucose transporter isoform GLUT1 (Fig. 5C, *middle* immunoblot) or the TnFR (Fig. 5C, *bottom* immunoblot), indicating normal cellular endocytic retrieval. In contrast, the same samples re-

Fig. 5. Cr Does Not Affect Plasma Membrane or Caveolae Integrity, or Elicit GLUT1 or TnFR Accumulation in the Plasma Membrane

    Treatments and methods performed as described in preceding legends. A, Propidium iodide staining; B, caveolin-1 immunofluorescence; and C, plasma membrane fractions were resolved and immunoblotted for GLUT4, GLUT1, and TnFR. These are representative observations from three separate experiments. IF, Immunofluorescence.

vealed Cr was effective in enhancing GLUT4 translocation to the plasma membrane (Fig. 5C, *top* immunoblot). These data are consistent with the increase in the basal-state plasma membrane level of GLUT4 resulting from GLUT4-containing vesicle exocytosis as previously observed (30) and not as a result of impaired endocytic retrieval. Also, shown here is a specific effect of Cr on GLUT4, but not GLUT1 or TnFR.

Cr Enhances Insulin-Stimulated, But Not Basal, Glucose Transport

Improved insulin sensitivity in individuals with type 2 diabetes has been demonstrated with 200-1000 μg/d (3.84 to 19.2 μmol) of Cr as CrPic (36, 37). To put this supplemental Cr dose in perspective, the average weight of those Cr-supplemented individuals was 70 kg. Assuming an extracellular fluid volume of approximately 11 liters, this corresponds to 350-1748 nM. Considering that CrPic is absorbed with approximately 2–5% efficiency (38), the predicted absorbed extracellular concentration would range between 7 and 87.4 nM. As we have observed, exposure of cells to the highest CrPic concentration tested (10 μM) increased the basal and insulin-stimulated levels of GLUT4 in the plasma membrane (Fig. 6A, compare panels 1 and 5, and 6 and 10). To our surprise, a 1000-fold lower concentration of CrPic (10 nM) also appeared to enhance the basal and insulin-stimulated levels of GLUT4 in the plasma membrane (Fig. 6A, compare panels 1 and 2, and 6 and 7). Inductively coupled plasma mass spectrometry indicated that our media contained approximately 1 nM Cr and, accordingly, GLUT4 translocation was not induced by treatment of

cells with 1 nM CrPic (data not shown). We confirmed these qualitative immunofluorescent data by subjecting detergent solubilized plasma membrane fractions to Western immunoblot analysis for GLUT4. Data from these biochemical analyses substantiate that basal and insulin-stimulated GLUT4 translocation is increased by 10 nM CrPic treatment (Fig. 6B, immunoblot). Densitometric analysis of GLUT4 band intensity from three subcellular fractionation experiments show basal and insulin-stimulated GLUT4 translocation is increased by 10 nM CrPic treatments (Fig. 6B, graph).

    Next, we tested the activity of these transporters by assessing the effect of CrPic on basal and insulin-stimulated 2-deoxyglucose uptake. In the absence of CrPic, insulin significantly increased ($P <0.05$) glucose transport (Fig. 6C). In striking contrast to the observed CrPic effect on GLUT4 translocation, a concomitant CrPic-induced increase in 2-deoxyglucose uptake was not seen at any dose tested (Fig. 6C). However, insulin-stimulated glucose transport was significantly enhanced in cells pretreated with CrPic (Fig. 6C). The lack of noninsulin-stimulated glucose transport by the Cr-mobilized pool of GLUT4 could be explained if these transporters were not physically incorporated into the plasma membrane, as suggested by the recurring observation (see Figs. 1 and 6) that the basal-state plasma membrane level of GLUT4 induced by chromium was less in highly purified membrane sheets than centrifuged-fractions. A possible explanation could be that sheets prepared by sonication lack tethered and/or docked GLUT4, but a fraction of this population of GLUT4 may be present in the plasma membrane pool collected by differential centrifugation. If true, this would mechanistically explain the lack

A IF: GLUT4
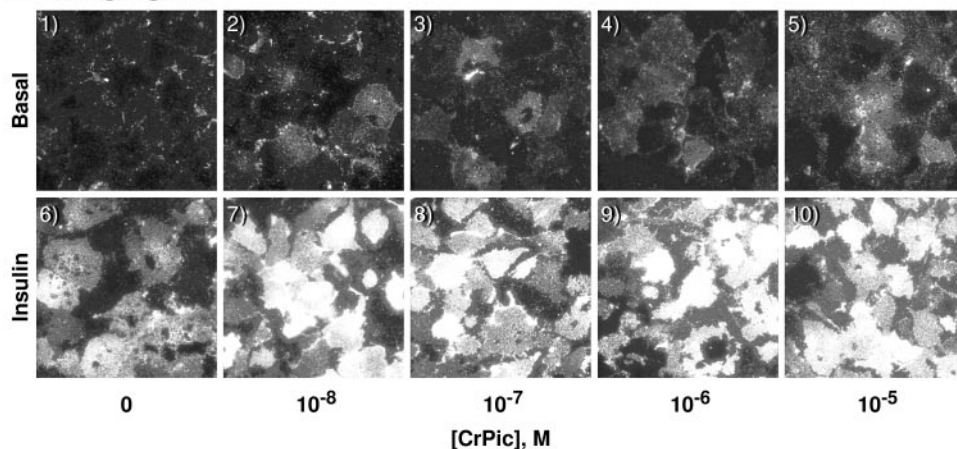
B IB: GLUT4
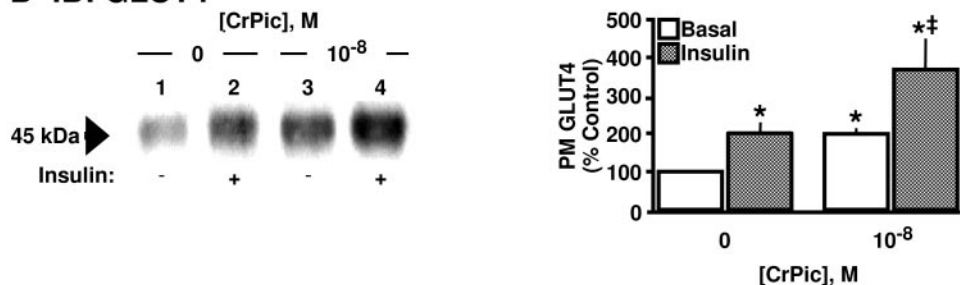
C Glucose Transport
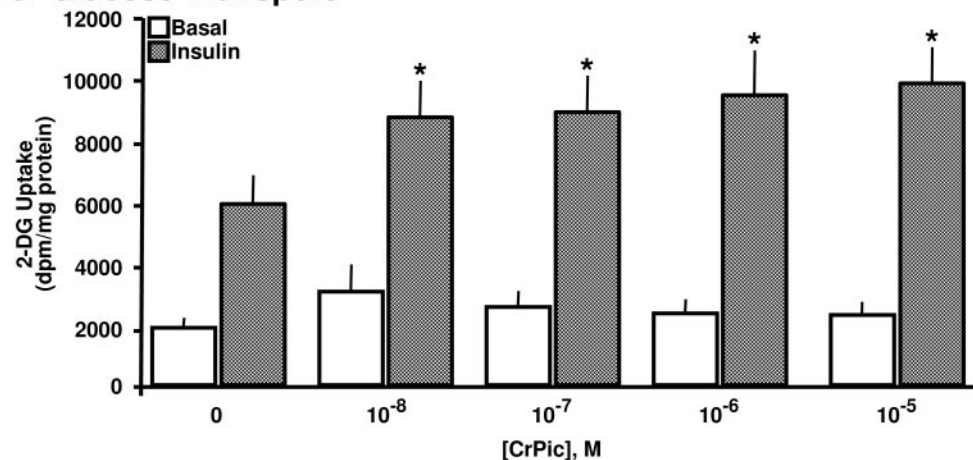
Fig. 6. Pharmacological Effects of Cr on GLUT4 and Glucose Transport

Cells were treated with the indicated doses of CrPic in serum-free DMEM for 16 h, and left unstimulated and stimulated with insulin as described in preceding legends. A, Representative PM sheet GLUT4 images are shown from three experiments. B, Representative PM fraction subjected to GLUT4 immunoblotting and densitometry quantification of band intensity (mean ± SE; *, $P < 0.05$ *vs.* basal without Cr; ‡, $P < 0.05$ *vs.* basal with Cr) from three separate experiments are expressed as percent of control. C, Glucose transport was determined by specific uptake of 2-[³H]deoxyglucose as described in *Materials and Methods*. They represent the mean (±SE; *, $P < 0.05$ *vs.* insulin without Cr) from seven to 10 independent experiments. All insulin-stimulated uptakes were significantly ($P < 0.001$) elevated over their respective controls. IF, Immunofluorescence.

of function of the chromium-mobilized pool of transporters.

To directly test this postulate that CrPic increases tethered and/or docked nonfunctional GLUT4 at the

cell surface, we expressed Myc-GLUT4-EGFP [enhanced green fluorescent protein (GFP)] with the Myc epitope of this protein in its exofacial loop and with EGFP at its carboxy terminus. The Myc epitope can be

detected when on the cell surface by probing unpermeabilized cells with the combination of a monoclonal anti-Myc antibody and a rhodamine-labeled anti-mouse IgG. In the basal state lacking CrPic, Myc-GLUT4-EGFP was predominantly localized to the perinuclear region and staining these cells for the Myc-tag without permeabilization demonstrated the lack of plasma membrane incorporation of this transporter (Fig. 7A, panel 1). As expected, treatment of cells with insulin resulted in a clear translocation of Myc-GLUT4-EGFP to the plasma membrane as depicted by the coappearance of both the rhodamine-labeled Myc- and EGFP-tag in nonpermeabilized cells at the cell surface (Fig. 7A, panel 2). In marked contrast, CrPic treatment alone resulted in an accumulation of GLUT4 at the inner surface of the plasma membrane that was not contiguous with the plasma membrane (Fig. 7A, panel 3). This redistribution occurred concomitant with an increase in small vesicular structures scattered throughout the cell cytoplasm. In the presence of insulin treatment, the CrPic-mobilized pool of GLUT4 was incorporated into the plasma membrane as depicted by the overlap between the GLUT4-EGFP and Myc-rhodamine signals (Fig. 7A, panel 4). Quantitation of the number of cells displaying these two phenotypes demonstrated that CrPic treatment resulted in a large increase in the number of cells with a subplasma membrane punctate distribution (Fig. 7B, compare *open bars*). Insulin stimulation significantly decreased the number of control and CrPic-treated cells displaying a subplasma membrane punctate distribution (Fig. 7B, *stippled bars*). Concomitant with this insulin-stimulated loss of punctate cells, the percent of cells showing plasma membrane Myc staining was significantly increased by insulin in the absence or presence of CrPic (Fig. 7C). In agreement with the 30% amplification of insulin-stimulated glucose transport by chromium (Fig. 6C), CrPic increased the insulin-stimulated plasma membrane level of GLUT4 by 38% ($P < 0.001$) as quantified by the ratio between intensities of rhodamine B on the cell surface and total EGFP in cells expressing Myc-GLUT4-EGFP (Fig. 7D). This percent increase is comparable to the chromium-induced increase in insulin-stimulated plasma membrane GLUT4 determined via the sheet assay.

Finally, because CrPic treatment was not associated with an amplification of the insulin signal (Fig. 2), we assessed whether the augmented action of insulin to stimulate glucose transport in the presence of 10 nM CrPic was due to the cholesterol-dependent increase in GLUT4 at the cell surface. Figure 8 shows that this pharmacological dose of CrPic significantly decreased the basal-state plasma membrane level of cholesterol (Fig. 8A). The reduction in plasma membrane cholesterol induced by CrPic treatment was prevented in cells incubated in medium enriched with βCD:Chol (Fig. 8A). The effect of βCD:Chol did not significantly alter the basal-state plasma membrane level of cholesterol (Fig. 8A). Consistent with the beneficial effect of CrPic on insulin action being due to the cholesterol-

dependent mobilized pool of GLUT4, the ability of CrPic to enhance insulin-stimulated glucose transport was prevented in cells incubated in βCD:Chol (Fig. 8B). Also, βCD:Chol alone did not alter basal and insulin-stimulated glucose transport.

DISCUSSION

We found that Cr, an essential transition metal suggested as being beneficial in individuals with glucose intolerance, type 2 diabetes, gestational diabetes, and steroid-induced diabetes, shows evidence of enhancing insulin action and glucose transport at the molecular level. In particular, our studies show that CrPic treatment recruits intracellular localized GLUT4 to a region juxtaposed to the cytoplasmic side of the plasma membrane. However, in the presence of insulin treatment, these subplasma membrane-localized transporters fuse to the plasma membrane and enhance insulin-stimulated glucose transport. Mechanistically, our data reveal that the beneficial action of CrPic on GLUT4 redistribution is cholesterol dependent. In this regard, it is interesting that Cr treatment is associated with drops in elevated circulating cholesterol and triglyceride concentrations in obese and type 2 diabetic rats (3, 39) and type 2 diabetic subjects (37, 40). Our findings provide novel molecular insight by which Cr supplementation might be beneficial for individuals with impaired glucose and lipid metabolism.

Data from our group shows that cholesterol depletion not associated with disruption in caveolae structure or insulin action activates GLUT4 translocation (30). Interestingly, as observed with the cholesterol-dependent action of chromium in the present work, cell surface-localized GLUT4 induced by βCD does not increase basal glucose transport (41). Combined, these data predict that changes in plasma membrane lipid biochemistry regulate GLUT4 recruitment to the plasma membrane. Our data also show that this CrPic-mobilized pool of GLUT4 incorporates into the plasma membrane with insulin stimulation and that this event results in an amplified insulin effect.
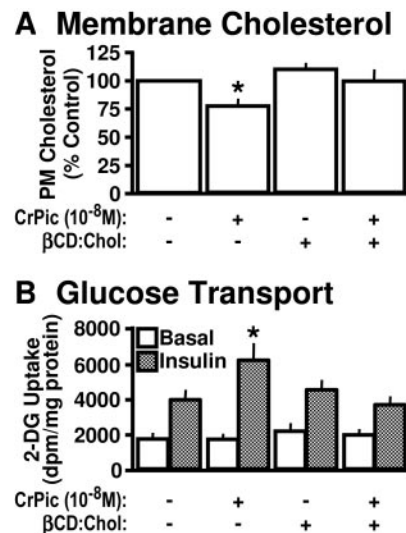
The mechanism by which CrPic decreases cholesterol is speculative but may occur by means similar to that used by the antidiabetic drug metformin. For example, metformin has recently been reported to activate 5′-AMP-activated kinase (AMPK) (42, 43). Metformin-stimulated AMPK activity has been shown to suppress expression of a sterol regulatory element binding protein, SREBP-1 (43), which belongs to a family of key lipogenic transcription factors directly involved in the expression of more than 30 genes dedicated to the synthesis and uptake of cholesterol, fatty acids, triglycerides, and phospholipids, as well as the reduced nicotinamide adenine dinucleotide phosphate cofactor required to synthesize these molecules (44). Although AMPK plays a role in contraction- and hypoxia-regulated glucose transport in skeletal mus-
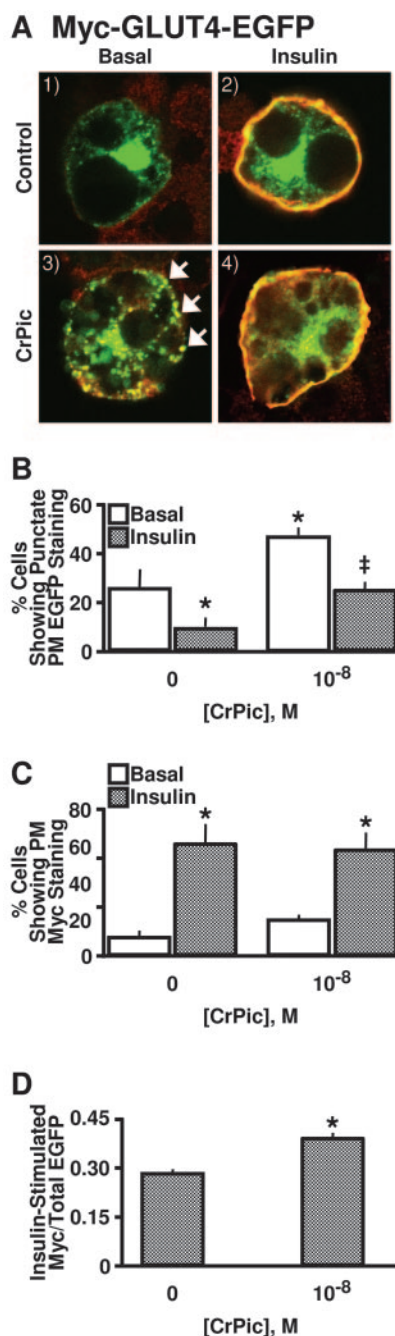
Fig. 7. GLUT4 at the Cell Surface Is Increased by Cr, but These Transporters Are Not Plasma Membrane Incorporated in the Absence of Insulin

3T3-L1 adipocytes were electroporated with Myc-GLUT4-EGFP cDNA. After reseeding for 20 h, cells were serum-starved in the absence (Control) or presence of 10^{-8} M CrPic for 16 h and then treated as described in preceding legends. Cell surface Myc-GLUT4-EGFP was detected with antimonoclonal anti-Myc antibody as described in *Materials and Methods*. A, Cells were then subjected to immunofluorescence microscopy with an antibody that recognizes the Myc epitope. Cell surface localized Myc-GLUT4-EGFP not physically incorporated into the plasma membrane are denoted with *arrows*. Representative observations from nine independent experiments are shown; B, percent cells displaying punctate EGFP staining at the cell surface; and C, percent cells displaying plasma membrane Myc staining. Data presented are the pooled results (mean ± SE) from nine independent experiments in which 100 cells from each group were blindly scored as either punctate EGFP or plasma membrane fused Myc. (*, $P < 0.05$ *vs.* basal without Cr; ‡, $P < 0.05$ *vs.* basal with Cr). D, The ratio between the Myc immunofluorescence and total EGFP signal intensities in insulin-stimulated Myc-GLUT4-EGFP-expressing cells pretreated in the absence or presence of CrPic. Data presented are from the analysis of 10 cells. *, $P < 0.05$.

Fig. 8. Cr-Enhanced Insulin-Stimulated Glucose Transport Is Cholesterol Dependent

3T3-L1 adipocytes were pretreated in the absence (−) or presence (+) of 10^{-8} M CrPic for 16 h in serum-free media which did not (−) or did contain (−) 1 mM βCD preloaded with cholesterol. A, Cells were harvested, plasma membrane fractions were prepared, and membrane cholesterol content was determined as described in *Materials and Methods*. Results are expressed as percent of control. They represent the mean (±SE; *, $P < 0.05$) from three independent experiments. B, Glucose transport was determined by specific uptake of 2-[^{3}H]deoxyglucose as described in *Materials and Methods*. All insulin-stimulated uptakes were significantly ($P < 0.001$) elevated over their respective controls. *, $P < 0.05$ *vs.* all other groups.

cle, it does not have this insulin mimetic action in 3T3-L1 adipocytes (45–47). Nonetheless, given that AMPK is expressed and activated by 5-aminoimidazole-4 carboxamide ribonucleoside (AICAR) in 3T3-L1 adipocytes (45, 46), the reduction in plasma membrane cholesterol we observe in adipocytes after exposure to CrPic may result from an AMPK effect. In keeping with this possibility, we have observed that treatment of 3T3-L1 adipocytes with CrPic induces AMPK Thr172 phosphorylation (data not shown). Although studies aimed at dissecting the interrelationships between AMPK and cholesterol biosynthesis in 3T3-L1 adipocytes requires further attention, a role for

Cr-induced AMPK activity in directly enhancing insulin action is difficult to reconcile given that AICAR, in contrast to CrPic, inhibits insulin-stimulated GLUT4 translocation and glucose transport in 3T3-L1 adipocytes (45). Moreover, plasma membrane sheets from AICAR-treated cells fail to show an AMPK effect on basal GLUT4 translocation in 3T3-L1 adipocytes (45). Nevertheless, a recent study visualized AICAR-stimulated translocation of GLUT4-EGFP in 3T3-L1 adipocytes (48). Based on our findings, a potential explanation to this published discrepancy may be that AICAR mobilizes GLUT4 to the cell surface (as visualized by GLUT4-EGFP) but does not significantly enhance GLUT4-containing vesicle and plasma membrane fusion (as accounted by examination of plasma membrane sheets containing little, if any, nonfused GLUT-4-containing vesicles).

Apart from learning how CrPic treatment leads to a reduction in plasma membrane cholesterol, an aspect of our ongoing work is aimed at understanding how membrane cholesterol loss recruits intracellular GLUT4 to the plasma membrane. It is well established that activation of GLUT4 translocation by insulin requires a PI3K signal involving the upstream IR and IRS activators and the downstream Akt-2 enzyme. Also, studies suggest that a second pathway occurs as a consequence of Cbl tyrosine phosphorylation (49–51), although this is somewhat controversial (52). As we recently reported for other cholesterol-dependent insulin mimetic agents (30), the basal and insulin-stimulated activities of these signaling molecules were not affected by CrPic treatment. Certainly, CrPic may engage the insulin signaling network distal to the molecules examined here, or it remains formally possible that Cr-induced GLUT4 redistribution is engaged by a noninsulin signaling pathway. For example, with the exception of IGF-I and IGF-II, a substantial amount of data suggest that many noninsulin stimuli (*e.g.* contraction, hypoxia, nitric oxide, phorbol ester, β- and α-adrenergic agonists, and $G_{q/11}$-coupled receptors) regulate GLUT4 translocation by engaging PI3K-independent signaling mechanisms (53). A common finding from study of many different insulin mimetic stimuli is the necessity of tyrosine kinase activity (53). Interestingly, recent evidence suggests that redistribution of raft domain components induces a tyrosine kinase-dependent insulin mimetic signal in rat adipocytes (54). In particular, synthetic intracellular caveolin binding domain peptide derived from caveolin-associated pp59[Lyn] or exogenous phosphoinositolglycan derived from glycosyl phosphatidylinositol membrane protein anchor (phosphoinositolglycan) triggers a concentration-dependent release of caveolar components and the glycosyl phosphatidylinositol-anchored protein Gce1, as well as the nonreceptor tyrosine kinases pp59[Lyn] and pp125[Fak], from interaction with caveolin (54). This dissociation, which parallels redistribution of the components from raft to nonraft areas of the adipocyte plasma membrane, is accompanied by tyrosine phosphorylation and activation of pp59[Lyn] and pp125[Fak] but not of the IR. In support of Cr targeting pp59[Lyn], Vasant *et al.* (55) recently observed that treatment of lymphocytes with Cr led to the activation of Src-family protein tyrosine kinases. Nonetheless, we do not detect an increase in the tyrosine phosphorylation of pp59[Lyn] or pp125[Fak] (data not shown). Also, incompatible with a signaling role of pp59[Lyn] or pp125[Fak] in Cr-stimulated GLUT4 translocation is the observation that these molecules have an insulin-mimetic action by increasing the tyrosine phosphorylation of IRS1 (54), an event not elicited by Cr in the present study.

Inconsistent with the notion that Cr enhances insulin action via amplifying insulin signal transduction, we present evidence that Cr favorably influences insulin action by a novel cholesterol-dependent mechanism augmenting the level of GLUT4 juxtaposed to the plasma membrane. Although we are continuing to explore signal transduction possibilities, we favor the idea that Cr action mechanically extends from cholesterol-dependent rafts to the actin cytoskeleton. Recent studies have shown that the lipid second messenger phosphatidylinositol (4, 5) bisphosphate, $PI(4,5)P_2$, accumulates at rafts where it regulates actin dynamics at the cell surface (56, 57). Thus, an emerging theme in the field of raft biology is that the changes in raft function are tightly coupled to actin cytoskeletal mechanics. A role for actin in insulin-stimulated GLUT4 translocation has been implicated by several studies (58–62). Thus, further study exploring whether a possible mechanistic explanation for Cr action on GLUT4 trafficking may involve actin cytoskeletal events is necessary. In any case, the findings reported here strengthen the association between insulin and Cr action and support the improvements on glucose and lipid metabolism.

The nonsignaling molecular findings herein are more in harmony with clinical observations that Cr has no effect on glucose control in healthy subjects, because if Cr action was attributed to signal amplification, the predicted upshot would be a drop in blood glucose regardless of an individual's glycemic state. We propose that Cr may selectively enhance the ability of insulin to stimulate glucose transport in cells rendered insulin resistant because of abnormal lipid parameters (*i.e.* increased plasma membrane cholesterol). In support of this model, recent study has revealed that erythrocyte membrane phospholipid composition is related to insulin resistance in obese nondiabetic women (63). In particular, insulin-resistant overweight women had significantly higher membrane sphingomyelin and cholesterol contents than lean women, and weight loss intervention induced an improvement of membrane lipid composition and insulin sensitivity. We believe that continued clinical study, as well as functional studies, are highly merited and required to elucidate the molecular basis and clinical relevance of Cr supplementation.

MATERIALS AND METHODS

Antibodies, Plasmids, and Reagents

Polyclonal rabbit caveolin-1 antibody and horseradish peroxidase-conjugated goat antirabbit and antimouse antibodies were obtained from Santa Cruz Biotechnology (Santa Cruz, CA). Polyclonal rabbit phospho-Akt (Ser473) and phospho-Cbl (Tyr774) antibodies were purchased from Cell Signaling Technology (Beverly, MA). Polyclonal rabbit GLUT1 antibody was obtained from Biogenesis (Kingston, NH). Monoclonal mouse transferrin receptor antibody was obtained from Zymed Laboratories (San Francisco, CA). Monoclonal phosphotyrosine antibody (PY20:horseradish peroxidase) was purchased from BD Transduction Laboratories (Lexington, KY). Rhodamine red-X-conjugated donkey antirabbit or antimouse antibodies were from Jackson ImmunoResearch (West Grove, PA). Anti-Akt 2-specific antibody was a generous gift from Dr. Morris J. Birnbaum (University of Pennsylvania, Philadelphia, PA). Polyclonal rabbit GLUT4 antibody and EGFP-tagged GLUT4 were kindly provided by Dr. Jeffrey E. Pessin (State University of New York at Stony Brook, Stony Brook, NY). DMEM was from Invitrogen (Grand Island, NY). FBS and FCS were obtained from Hyclone Laboratories Inc. (Logan, UT). CrPic was from Tokyo Kasei Kogyo Co. (Tokyo, Japan). Insulin and all other chemicals were from Sigma (St. Louis, MO).

Cell Culture and Treatments

Murine 3T3-L1 preadipocytes were purchased from American Type Culture Collection (Manassas, VA). Murine 3T3-L1 preadipocytes were cultured in DMEM containing 25 mM glucose and 10% calf serum at 37 C in an 8% CO_2 atmosphere. Confluent cultures were induced to differentiate into adipocytes as previously described (30). All studies were performed on adipocytes, which were between 8 and 12 d after differentiation. Transfection experiments were performed with 50 μg of GFP-tagged plasmid DNA for analysis of GFP fluorescence as previously described (30). After electroporation, the adipocytes were plated on glass coverslips and allowed to recover for 16–18 h before use. The cells were treated with certain concentrations of $CrCl_3$ and CrPic in serum-free DMEM for 16 h. During the last 5 or 30 min of incubation, the cells were either left unstimulated or stimulated with 1 or 100 nM insulin as indicated. The preparation of βCD:Cholesterol complex was performed essentially by the method of Christian *et al.* (64), with minor modifications as previously described (30). In the cholesterol replenishment experiments, cells were incubated with this solution for 30 min before insulin treatment.

Plasma Membrane Sheet Assay

Preparation of plasma membrane sheets from the adipocytes was as previously described (30). After the isolation of plasma membrane sheets, these purified membranes were used for immunofluorescence. The sheets were fixed for 20 min at 25 C in a solution containing 2% paraformaldehyde, 70 mM KCl, 30 mM HEPES (pH 7.5), 5 mM $MgCl_2$, and 3 mM EGTA. The sheets were then blocked in 5% donkey serum for 60 min at 25 C and incubated for 60 min at 25 C with a 1:1000 dilution of polyclonal rabbit GLUT4 antibody, 1:100 dilution of polyclonal rabbit GLUT1 antibody, 1:50 dilution of polyclonal rabbit caveolin-1 antibody, or 1:50 dilution of mouse transferrin receptor antibody, followed by incubation with a 1:50 dilution of rhodamine red-X-conjugated donkey antirabbit or antimouse IgG for 60 min at 25 C. The amount of glucose transporter on the plasma membrane was quantitated by digital image processing as described previously (31, 65). To ensure that quantitation was performed in an unbiased man-

ner, fields of sheets were selected based solely on their staining with fluorescein isothiocyanate (FITC)-conjugated phosphatidylethanolamine. Images of both the FITC- and rhodamine-stained sheets were acquired, and the regions to be quantitated were marked in the image captured with the FITC filter. These regions were then transferred to the image captured using the rhodamine filter, and the average pixel brightness of each marked sheet was determined.

Subcellular Fractionation

Plasma membrane fractions were obtained by using a differential centrifugation method previously described (30). Briefly, 3T3-L1 adipocytes were washed and resuspended in HES buffer [20 mM HEPES (pH 7.4), 1 mM EDTA, and 255 mM sucrose containing 1 mM phenylmethylsulfonyl fluoride, 10 μg/ml pepstatin, 10 μg/ml aprotinin, and 5 μg/ml leupeptin]. Cell lysates were prepared by shearing the cells through a 22-gauge needle 10 times. Lysates were then centrifuged at 19,000 $\times$ *g* for 20 min at 4 C. The crude plasma membrane pellet was centrifuged under same conditions again and resuspended in HES buffer and layered onto a 1.12 M sucrose cushion for centrifugation at 100,000 $\times$ *g* for 60 min. The plasma membrane layer was removed from the sucrose cushion and centrifuged at 40,000 $\times$ *g* for 20 min. Pelleted membrane was resuspended in a detergent-containing lysis buffer and assayed for soluble protein content.

Glucose Transport Assay

Cells were washed with KRPH buffer [5 mM Na_2HPO_4, 20 mM HEPES (pH 7.4), 1 mM $MgSO_4$, 1 mM $CaCl_2$, 136 mM NaCl, 4.7 mM KCl, and 1% BSA] and either untreated or stimulated as described in the figure legends. Glucose transport was determined at 37 C by incubation with 50 μM 2-deoxyglucose containing 0.5 μCi of 2-[^{3}H]deoxyglucose in the absence or presence of 10 μM cytochalasin B. The reaction was stopped after 10 min by washing the cells three times with ice-cold PBS. The cells were then solubilized in 1% Triton X-100 at 37 C for 30 min, and aliquots were subjected to scintillation counting.

Cholesterol Analyses

Plasma membrane pellets were resuspended in 0.25 ml of HES buffer, and cholesterol content was determined by using an enzymatic, colorimetric kit for the quantitative determination of total cholesterol (catalog no. 276-64909; Wako Chemicals, Richmond, VA) as previously described (30). Briefly, 0.2 ml of the resuspended plasma membrane pellet was vigorously mixed with 5 ml of chloroform-methanol (2:1, vol:vol) extraction solution for 10 min. The mixture was then centrifuged (3000 rpm, 10 min), and 0.3 ml of the supernatant was added to a glass tube and evaporated via a water bath at 100 C. The residue was reconstituted with 0.2 ml of an isopropanol-Triton X-100 solution (9:1, vol/vol), and 2 ml of a color reagent solution were added. After a 15-min incubation at 37 C, absorbance was measured at 600 nm.

Preparation of Total Cell Extracts

Cell extracts were prepared from 100-mm plates of 3T3-L1 adipocytes. Cells from each plate were washed two times with ice-cold PBS and scraped into 1 ml of ice-cold lysis buffer [25 mM Tris (pH 7.4), 50 mM NaF, 10 mM $Na_3P_2O_7$, 137 mM NaCl, 10% glycerol, and 1% Nonidet P-40] containing 2.0 mM phenylmethylsulfonyl fluoride, 2 mM Na_3VO_4, 5 μg/ml aprotinin, 10 μM leupeptin, and 1 μM pepstatin A by rotation for 15 min at 4 C. Insoluble material was separated from the soluble extract by microcentrifugation for 15 min at 4 C.

Protein concentration was determined, and samples were subjected directly to SDS-PAGE.

Electrophoresis and Immunoblotting

Whole cell lysates were separated by 7.5% SDS-PAGE, and plasma membrane fractions (GLUT4 analyses) were separated by 10% SDS-PAGE. The resolved proteins were transferred to Immobilon P membrane (Millipore, MA) or nitrocellulose membrane (GLUT4 analyses) and immunoblotted with a monoclonal phosphotyrosine antibody, a phosphotyrosine-specific Cbl antibody, a phosphoserine-specific Akt antibody, an anti-Akt 2-specific antibody, or a GLUT4 antibody. All immunoblots were subjected to ECL detection (Amersham, Piscataway, NJ).

Statistical Analysis

All values are presented as means $\pm$ SE. ANOVA was used to determine differences among groups. Where a significant difference was indicated, the Tukey test was used to determine significant differences between groups. $P < 0.05$ was considered to be statistically significant.

Acknowledgments

References

1. Striffler JS, Law JS, Polansky MM, Bhathena SJ, Anderson RA 1995 Chromium improves insulin response to glucose in rats. Metabolism 44:1314–1320
2. Morris BW, Gray TA, Macneil S 1993 Glucose-dependent uptake of chromium in human and rat insulin-sensitive tissues. Clin Sci (Lond) 84:477–482
3. Cefalu WT, Wang ZQ, Zhang XH, Baldor LC, Russell JC 2002 Oral chromium picolinate improves carbohydrate and lipid metabolism and enhances skeletal muscle Glut-4 translocation in obese, hyperinsulinemic (JCR-LA corpulent) rats. J Nutr 132:1107–1114
4. Striffler JS, Polansky MM, Anderson RA 1999 Overproduction of insulin in the chromium-deficient rat. Metabolism 48:1063–1068
5. Striffler JS, Polansky MM, Anderson RA 1998 Dietary chromium decreases insulin resistance in rats fed a high-fat, mineral-imbalanced diet. Metabolism 47:396–400
6. Fulop Jr T, Nagy JT, Worum I, Foris G, Mudri K, Varga P, Udvardy M 1987 Glucose intolerance and insulin resistance with aging—studies on insulin receptors and post-receptor events. Arch Gerontol Geriatr 6:107–115
7. Pessin JE, Thurmond DC, Elmendorf JS, Coker KJ, Okada S 1999 Molecular basis of insulin-stimulated GLUT4 vesicle trafficking. Location! Location! Location! J Biol Chem 274:2593–2596
8. Satoh S, Nishimura H, Clark AE, Kozka IJ, Vannucci SJ, Simpson IA, Quon MJ, Cushman SW, Holman GD 1993 Use of bismannose photolabel to elucidate insulin-regulated GLUT4 subcellular trafficking kinetics in rat adipose cells. Evidence that exocytosis is a critical site of hormone action. J Biol Chem 268:17820–17829
9. Jhun BH, Rampal AL, Liu H, Lachaal M, Jung CY 1992 Effects of insulin on steady state kinetics of GLUT4 subcellular distribution in rat adipocytes. Evidence of constitutive GLUT4 recycling. J Biol Chem 267:17710–17715
10. Czech MP, Buxton JM 1993 Insulin action on the internalization of the GLUT4 glucose transporter in isolated rat adipocytes. J Biol Chem 268:9187–9190
11. Mertz W 1969 Chromium occurrence and function in biological systems. Physiol Rev 49:163–239
12. Anderson RA, Polansky MM, Bryden NA, Bhathena SJ, Canary JJ 1987 Effects of supplemental chromium on patients with symptoms of reactive hypoglycemia. Metabolism 36:351–355
13. Vincent JB 1999 Mechanisms of chromium action: low-molecular-weight chromium-binding substance. J Am Coll Nutr 18:6–12
14. Davis CM, Vincent JB 1997 Chromium oligopeptide activates insulin receptor tyrosine kinase activity. Biochemistry 36:4382–4385
15. Evans GW, Bowman TD 1992 Chromium picolinate increases membrane fluidity and rate of insulin internalization. J Inorg Biochem 46:243–250
16. Kao AW, Ceresa BP, Santeler SR, Pessin JE 1998 Expression of a dominant interfering dynamin mutant in 3T3L1 adipocytes inhibits GLUT4 endocytosis without affecting insulin signaling. J Biol Chem 273:25450–25457
17. Kublaoui B, Lee J, Pilch PF 1995 Dynamics of signaling during insulin-stimulated endocytosis of its receptor in adipocytes. J Biol Chem 270:59–65
18. Wang B, Balba Y, Knutson VP 1996 Insulin-induced in situ phosphorylation of the insulin receptor located in the plasma membrane versus endosomes. Biochem Biophys Res Commun 227:27–34
19. Dombrowski L, Faure R, Marette A 2000 Sustained activation of insulin receptors internalized in GLUT4 vesicles of insulin-stimulated skeletal muscle. Diabetes 49:1772–1782
20. Czech MP 1980 Insulin action and the regulation of hexose transport. Diabetes 29:399–409
21. Pilch PF, Thompson PA, Czech MP 1980 Coordinate modulation of D-glucose transport activity and bilayer fluidity in plasma membranes derived from control and insulin-treated adipocytes. Proc Natl Acad Sci USA 77:915–918
22. Muller S, Denet S, Candiloros H, Barrois R, Wiernsperger N, Donner M, Drouin P 1997 Action of metformin on erythrocyte membrane fluidity in vitro and in vivo. Eur J Pharmacol 337:103–110
23. Wiernsperger NF 1999 Membrane physiology as a basis for the cellular effects of metformin in insulin resistance and diabetes. Diabetes Metab 25:110–127
24. Pryor PR, Liu SC, Clark AE, Yang J, Holman GD, Tosh D 2000 Chronic insulin effects on insulin signalling and GLUT4 endocytosis are reversed by metformin. Biochem J 348:83–91

25. Fischer Y, Thomas J, Rosen P, Kammermeier H 1995 Action of metformin on glucose transport and glucose transporter GLUT1 and GLUT4 in heart muscle cells from healthy and diabetic rats. Endocrinology 136:412–420

26. Hundal HS, Ramlal T, Reyes R, Leiter LA, Klip A 1992 Cellular mechanism of metformin action involves glucose transporter translocation from an intracellular pool to the plasma membrane in L6 muscle cells. Endocrinology 131:1165–1173

27. Morris B, Gray T, MacNeil S 1995 Evidence for chromium acting as an essential trace element in insulin-dependent glucose uptake in cultured mouse myotubes. J Endocrinol 144:135–141

28. Joost HG, Schurmann A 2001 Subcellular fractionation of adipocytes and 3T3-L1 cells. Methods Mol Biol 155:77–82

29. Vincent JB 2000 The biochemistry of chromium. J Nutr 130:715–718

30. Liu P, Leffler BJ, Weeks LK, Chen G, Bouchard CM, Strawbridge AB, Elmendorf JS 2003 Sphingomyelinase activates GLUT4 translocation via a cholesterol-dependent mechanism. Am J Physiol Cell Physiol 286:C317–C329

31. Strawbridge AB, Elmendorf JS 2005 Phosphatidylinositol 4,5-bisphosphate reverses endothelin-1-induced insulin resistance via an actin-dependent mechanism. Diabetes 54:1698–1705

32. Niswender KD, Morrison CD, Clegg DJ, Olson R, Baskin DG, Myers MG Jr, Seeley RJ, Schwartz MW 2003 Insulin activation of phosphatidylinositol 3-kinase in the hypothalamic arcuate nucleus: a key mediator of insulin-induced anorexia. Diabetes 52:227–231

33. Chen R, Kang VH, Chen J, Shope JC, Torabinejad J, DeWald DB, Prestwich GD 2002 A monoclonal antibody to visualize PtdIns(3,4,5)P(3) in cells. J Histochem Cytochem 50:697–708

34. Tanaka K, Horiguchi K, Yoshida T, Takeda M, Fujisawa H, Takeuchi K, Umeda M, Kato S, Ihara S, Nagata S, Fukui Y 1999 Evidence that a phosphatidylinositol 3,4,5-trisphosphate-binding protein can function in nucleus. J Biol Chem 274:3919–3922

35. Subtil A, Gaidarov I, Kobylarz K, Lampson MA, Keen JH, McGraw TE 1999 Acute cholesterol depletion inhibits clathrin-coated pit budding. Proc Natl Acad Sci USA 96:6775–6780

36. Cefalu WT, Bell-Farrow AD, Stegner J, Wang ZQ, King T, Morgan T, Terry JG 1999 Effect of chromium picolinate on insulin sensitivity in vivo. J Trace Elem Exp Med 12:71–83

37. Anderson RA, Cheng N, Bryden NA, Polansky MM, Chi J, Feng J 1997 Elevated intakes of supplemental chromium improve glucose and insulin variables in individuals with type 2 diabetes. Diabetes 46:1786–1791

38. Vincent JB 2000 Quest for the molecular mechanism of chromium action and its relationship to diabetes. Nutr Rev 58:67–72

39. Sun Y, Clodfelder BJ, Shute AA, Irvin T, Vincent JB 2002 The biomimetic [Cr(3)O(O(2)CCH(2)CH(3))(6)(H(2)O)(3)](+) decreases plasma insulin, cholesterol, and triglycerides in healthy and type II diabetic rats but not type I diabetic rats. J Biol Inorg Chem 7:852–862

40. Lee NA, Reasner CA 1994 Beneficial effect of chromium supplementation on serum triglyceride levels in NIDDM. Diabetes Care 17:1449–1452

41. Parpal S, Karlsson M, Thorn H, Stralfors P 2001 Cholesterol depletion disrupts caveolae and insulin receptor signaling for metabolic control via insulin receptor substrate-1, but not for mitogen-activated protein kinase control. J Biol Chem 276:9670–9678

42. Musi N, Hirshman MF, Nygren J, Svanfeldt M, Bavenholm P, Rooyackers O, Zhou G, Williamson JM, Ljunqvist O, Efendic S, Moller DE, Thorell A, Goodyear LJ 2002 Metformin increases AMP-activated protein kinase ac-

tivity in skeletal muscle of subjects with type 2 diabetes. Diabetes 51:2074–2081

43. Zhou G, Myers R, Li Y, Chen Y, Shen X, Fenyk-Melody J, Wu M, Ventre J, Doebber T, Fujii N, Musi N, Hirshman MF, Goodyear LJ, Moller DE 2001 Role of AMP-activated protein kinase in mechanism of metformin action. J Clin Invest 108:1167–1174

44. Brown MS, Goldstein JL 1997 The SREBP pathway: regulation of cholesterol metabolism by proteolysis of a membrane-bound transcription factor. Cell 89:331–340

45. Salt IP, Connell JM, Gould GW 2000 5-aminoimidazole-4-carboxamide ribonucleoside (AICAR) inhibits insulin-stimulated glucose transport in 3T3-L1 adipocytes. Diabetes 49:1649–1656

46. Sakoda H, Ogihara T, Anai M, Fujishiro M, Ono H, Onishi Y, Katagiri H, Abe M, Fukushima Y, Shojima N, Inukai K, Kikuchi M, Oka Y, Asano T 2002 Activation of AMPK is essential for AICAR-induced glucose uptake by skeletal muscle but not adipocytes. Am J Physiol Endocrinol Metab 282:E1239–E1244

47. Mu J, Brozinick Jr JT, Valladares O, Bucan M, Birnbaum MJ 2001 A role for AMP-activated protein kinase in contraction- and hypoxia-regulated glucose transport in skeletal muscle. Mol Cell 7:1085–1094

48. Yamaguchi S, Katahira H, Ozawa S, Nakamichi Y, Tanaka T, Shimoyama T, Takahashi K, Yoshimoto K, Imaizumi MO, Nagamatsu S, Ishida H 2005 Activators of AMP-activated protein kinase enhance GLUT4 translocation and its glucose transport activity in 3T3-L1 adipocytes. Am J Physiol Endocrinol Metab 289:E643–E649

49. Liu J, DeYoung SM, Hwang JB, O'Leary EE, Saltiel AR 2003 The roles of Cbl-b and c-Cbl in insulin-stimulated glucose transport. J Biol Chem 278:36754–36762

50. Ribon V, Printen JA, Hoffman NG, Kay BK, Saltiel AR 1998 A novel, multifuntional c-Cbl binding protein in insulin receptor signaling in 3T3-L1 adipocytes. Mol Cell Biol 18:872–879

51. Baumann CA, Ribon V, Kanzaki M, Thurmond DC, Mora S, Shigematsu S, Bickel PE, Pessin JE, Saltiel AR 2000 CAP defines a second signalling pathway required for insulin-stimulated glucose transport. Nature 407:202–207

52. Mitra P, Zheng X, Czech MP 2004 RNAi-based Analysis of CAP, Cbl, and CrkII Function in the Regulation of GLUT4 by Insulin. J Biol Chem 279:37431–37435

53. Elmendorf JS 2002 Signals that regulate GLUT4 translocation. J Membr Biol 190:167–174

54. Muller G, Jung C, Wied S, Welte S, Jordan H, Frick W 2001 Redistribution of glycolipid raft domain components induces insulin-mimetic signaling in rat adipocytes. Mol Cell Biol 21:4553–4567

55. Vasant C, Rajaram R, Ramasami T 2003 Apoptosis of lymphocytes induced by chromium(VI/V) is through ROS-mediated activation of Src-family kinases and caspase-3. Free Radic Biol Med 35:1082–1100

56. Frey D, Laux T, Xu L, Schneider C, Caroni P 2000 Shared and unique roles of CAP23 and GAP43 in actin regulation, neurite outgrowth, and anatomical plasticity. J Cell Biol 149:1443–1454

57. Laux T, Fukami K, Thelen M, Golub T, Frey D, Caroni P 2000 GAP43, MARCKS, and CAP23 modulate PI(4,5)P(2) at plasmalemmal rafts, and regulate cell cortex actin dynamics through a common mechanism. J Cell Biol 149:1455–1472

58. Omata W, Shibata H, Li L, Takata K, Kojima I 2000 Actin filaments play a critical role in insulin-induced exocytotic recruitment but not in endocytosis of GLUT4 in isolated rat adipocytes. Biochem J 346:321–328

59. Wang Q, Bilan PJ, Tsakiridis T, Hinek A, Klip A 1998 Actin filaments participate in the relocalization of phosphatidylinositol3-kinase to glucose transporter-containing compartments and in the stimulation of glucose uptake

in 3T3-L1 adipocytes. Biochem J [Erratum (1999) 341(Pt 3):861] 331:917–928

60. Tsakiridis T, Bergman A, Somwar R, Taha C, Aktories K, Cruz TF, Klip A, Downey GP 1998 Actin filaments facilitate insulin activation of the src and collagen homologous/mitogen-activated protein kinase pathway leading to DNA synthesis and c-fos expression. J Biol Chem 273:28322–28331

61. Kanzaki M, Watson RT, Hou JC, Stamnes M, Saltiel AR, Pessin JE 2002 Small GTP-binding protein TC10 differentially regulates two distinct populations of filamentous actin in 3T3L1 adipocytes. Mol Biol Cell 13:2334–2346

62. Bose A, Cherniack AD, Langille SE, Nicoloro SM, Buxton JM, Park JG, Chawla A, Czech MP 2001 G(α)11 signaling

through ARF6 regulates F-actin mobilization and GLUT4 glucose transporter translocation to the plasma membrane. Mol Cell Biol 21:5262–5275

63. Younsi M, Quilliot D, Al-Makdissy N, Delbachian I, Drouin P, Donner M, Ziegler O 2002 Erythrocyte membrane phospholipid composition is related to hyperinsulinemia in obese nondiabetic women: effects of weight loss. Metabolism 51:1261–1268

64. Christian AE, Haynes MP, Phillips MC, Rothblat GH 1997 Use of cyclodextrins for manipulating cellular cholesterol content. J Lipid Res 38:2264–2272

65. Hausdorff SF, Frangioni JV, Birnbaum MJ 1994 Role of p21ras in insulin-stimulated glucose transport in 3T3-L1 adipocytes. J Biol Chem 269:21391–21394